European Polymer Journal 49 (2013) 1975–1983

Contents lists available at SciVerse ScienceDirect

European Polymer Journal

journal homepage: www.elsevier.com/locate/europolj

Improved electrical and flow properties of conductive polyolefin blends: Modification of poly(ethylene vinyl acetate) copolymer/carbon black with ethylene–propylene copolymer

Thomas Gkourmpis [a,*], Christer Svanberg [a], Senthil K. Kaliappan [b,1], Walter Schaffer [b], Martin Obadal [b], Gottfried Kandioller [b], Davide Tranchida [b,*]

[a] Innovation & Technology, Borealis AB, SE-444 86 Stenungsund, Sweden
[b] Borealis Polyolefine GmbH, St.-Peter-Straße 25, 4021 Linz, Austria

ARTICLE INFO

Article history:
Received 16 November 2012
Received in revised form 19 February 2013
Accepted 4 March 2013
Available online 15 March 2013

Keywords:
EVA
Electrical properties
Carbon black
Atomic force microscopy

ABSTRACT

Carbon black (CB) based polymer nanocomposites exhibit percolation-type conductive behaviour. In this work, the electrical performance of a nanocomposite based on poly(ethylene vinyl acetate) (EVA) was studied. By introducing a second polymer and creating a system with three phases, the filler is localised in a single phase. This localisation has been seen to affect the overall morphology of both phases, indicating that despite the phase separation there is interaction between the two systems. Furthermore, by keeping the filler to polymer ratio constant on the EVA phase, we have managed to achieve improved electrical performance by reducing the overall percolation threshold while increasing the overall amount of the second polymer. Atomic Force Microscope (AFM) and Scanning Electron Microscope (SEM) imaging has been used to verify the preferential location of the conductive particles and to reveal the complex morphology developed. The results presented in this study show the possibility of specially-designed polymer compositions for conductive applications.

1. Introduction

Synthetic polymers are often very good electrically insulating materials and in order to make them conduct electricity, the preferred choice is to mix them with conductive fillers, like carbon black, graphite, carbon fibres, carbon nanotubes, metal particles, etc. Traditionally carbon black (CB) is the filler of choice for large-scale industrial processes, especially for cost reasons, and its addition to the polymer matrix can lead to a degree of electrical conductivity [1]. Such systems exhibit a percolation-type conductive behaviour [2–4], but introducing fillers into the polymer matrix has as well a profound effect, especially, on the mechanical properties as the material tends to become much tougher [5,6]. Depending on the filler and the required conductivity level unique materials can be designed, that are suitable for electromagnetic shielding, thermal resistors, automotive boards, power cable shielding, chemical vapour sensors and pipe applications [7–9]. The downside of this concept is that in order to achieve sufficient conductivity one normally needs high amounts of conductive filler that lead to a dramatic increase of the composition viscosity. This creates serious issues with respect to processing ability and performance [10].

For many simple binary systems the percolation threshold is 12–15 vol% filler [11,12], although it can be significantly lower or higher [13,14] depending on the conductivity level required. Lowering this percolation threshold appears to be an effective way of reducing the

* Corresponding authors. Tel.: +46 303 20 5576 (T. Gkourmpis), tel.: +43 732 6981 5917 (D. Tranchida).
E-mail addresses: thomas.gkourmpis@borealisgroup.com (T. Gkourmpis), davide.tranchida@borealisgroup.com (D. Tranchida).
[1] Current address: Goodyear Innovation Center, Colmar-Berg, Luxembourg.

0014-3057/$ - see front matter © 2013 Elsevier Ltd. All rights reserved.
http://dx.doi.org/10.1016/j.eurpolymj.2013.03.003

required amount of conductive filler and thus the processing-related problems, while keeping the all-important conductivity at adequate levels and minimising issues arising from mechanical properties. However, for binary systems (i.e. carbon black mixed with one polymer) there is a direct and intrinsic coupling between the electrical percolation, which gives a low conductivity, and the mechanical percolation, which reduces processing ability. One way to circumvent this relation is by addition of carbon black particles to an immiscible blend of two polymers [15–19]. With the proper choice of polymers and fillers, it becomes possible to force the filler localisation in one of the two phases, or on the interface between them [18], which allows to simultaneously obtain high conductivity and good processing ability.

A key factor for material properties is good dispersion and distribution that requires the filler to be mixed in an efficient manner. Mixing is thought to be determined by two distinct mechanisms, the initial interfacial localisation of the filler and the subsequent thermodynamically driven mixing in the preferred phase [20]. When the shear forces or the filler concentration increases, the possibility of movement towards one of the components of the blend is increased. Consequently diffusion of the fillers occurs from the polymer–polymer interface into the polymeric phase that is thermodynamically preferable [20]. Properties like polarity, oxidation and viscosity are thought to affect this preferential location. In industrial applications the filler levels can vary dramatically and the use of high power compounders ensure an abundance of shear forces and thus mobility in the polymer/polymer/filler system. Therefore it is expected that thermodynamics will play an important role in the location of the filler at the preferred polymeric phase.

In this paper we report on the material properties of a semi conductive blend of two polyolefin copolymers, poly(ethylene vinyl acetate) (EVA) and ethylene–propylene copolymer (EPP), mixed with carbon black. The microscopic and morphological properties are characterised using Atomic Force Microscopy (AFM) and Differential Scanning Calorimetry (DSC) and linked to the macroscopic resistivity and the flow properties of the melt. We show that the behaviour of these systems can be tuned such that materials with designed properties can be produced.

2. Experimental

The polymers used in this study were commercially available poly(ethylene vinyl acetate) (EVA) and Ethylene–Propylene Copolymer (EPP). Material characterisation has been performed via GPC and DSC and the results are reported in Table 1. The relevant information for the CB used is listed in Table 2.

Melt mixing was performed on a BUSS MKD 46B/15LD compounder at 170 °C at a screw speed of 210 rpm. Final blends were cooled down with water at room temperature and pelletized for easier use.

The compositions used in this study are listed in Table 3. In order to compare to a reference made of only EVA and CB, the relative contents of the three components was adjusted such that the weight ratio of EVA/CB is kept fixed at 60/40. In addition, 14 different EVA/CB blends with CB content in the range 27–40% were used as discussed in Fig. 1 of the results part for a first comparison.

The pellets were compression moulded into plates ~1 mm thick at 190 °C and cooled down to room temperature between two cold metal blocks. Samples were taken from the plates and cut under cryogenic conditions (−30 °C for EPP and −100 °C for all other samples) using a RMC – PowerTome PC (AZ, USA) ultra-cryo-microtome. Surfaces with RMS roughness of ca. 20 nm on a $5 \times 5\ \mu m^2$ were obtained and used for further morphological investigations by AFM.

AFM images were obtained using an Asylum Research MFP-3D (CA, USA) and analysed with Scanning Probe Image Processor SPIP (Imagemet, Denmark). The instrument was operated in AC mode with Olympus AC240TS cantilevers, nominal spring constant and resonance frequency of 2 N/m and 70 kHz respectively. Since the phase lag depends on dissipated energy, and this is related to a number of different factors as e.g. stiffness, adhesion, viscous force, it was not attempted to extract quantitative information out of the phase images. However, the experimental conditions were kept constant in order to be able to at least compare the phase images, step by step adding one component to the sample to be imaged. Therefore, a large free amplitude (100 nm) was used for all the experiments, with setpoint (ratio of the free and feedbacked amplitude) of 0.73.

Resistivity was measured on string samples obtained during mixing using an HP/Agilent 4339A High Resistance Meter. The volume resistivity (VR) was obtained as:

$$VR = RA/L \quad (1)$$

where R is the measured resistance, A the cross-section area and L the length of the sample respectively.

Differential Scanning Calorimetry was performed with a TA Q2000 instrument, calibrated with indium. Heating and cooling scans were performed at 10 K/min on approximately 5 mg samples.

Scanning Electron Microscopy (SEM) was performed using a FEI Quanta 200F microscope. Analysis of the samples stained with RuO_4 was performed under low vacuum conditions with an acceleration voltage of 8 kV. Specimens

Table 1
Description of the polymers used in this work. Tm and TC are the melt and crystallisation temperatures respectively. Tacticity was measured by NMR.

Material	M_w	M_n	Degree of crystallinity (%)	T_m (°C)	T_C (°C)	Melt index	VA content (wt%)	Ethylene content (wt%)	Tacticity (%)
EPP	17,000	8000	17.2	80.1	43.1	>100		8.6	21.78
EVA	161,000	14,000	36	81.7	64.5	20	20		

Table 2
Description of the carbon black used in this work.

BET (m^2/g)	Mean particle size (nm)	OAN (cc/100 g)	Iodine number (g/kg)
42	56	121	43

Table 3
Sample compositions.

Sample	EVA (wt%)	EPP (wt%)	CB (wt%)
EVA/CB	60	0	40
EVA/5%EPP/CB	57	5	38
EVA/10%EPP/CB	54	10	36
EVA/30%EPP/CB	42	30	28
EVA	100	0	0
EPP	0	100	0
EVA/EPP	50	50	0

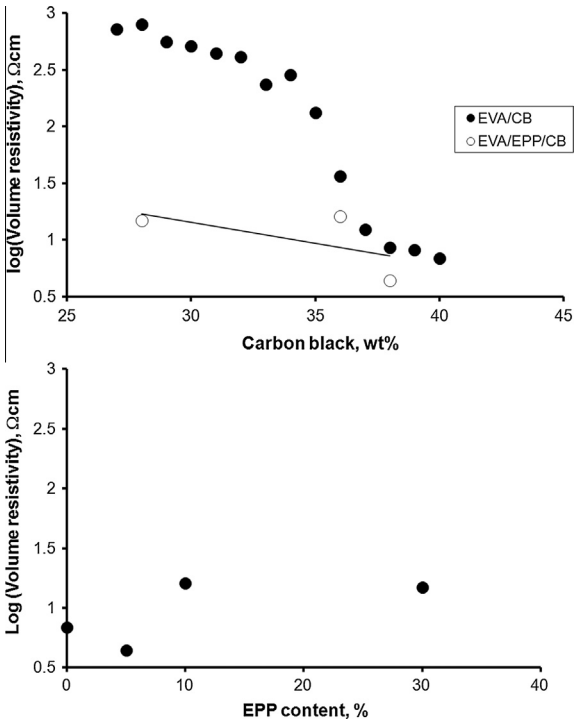

Fig. 1. Volume resistivity as a function of CB loading for a system containing only EVA/CB and EVA/EPP/CB. Lines are a guide to the eye.

for RuO_4 staining were trimmed under cryo-conditions. RuO_4 was produced in situ by adding $RuCl_3$ to a saturated $NaIO_4$ solution. Staining of the specimens was conducted in the vapour phase for 6 h. After washing with distilled water and subsequent drying, a top layer of approximately 3 μm was removed from the stained specimens by room temperature ultra-microtomy prior to SEM analysis.

3. Results and discussion

In order to first check for the effect of CB content, the electrical behaviour of a series of pure EVA mixed with CB is compared in Fig. 1 with EVA/EPP blends with varying concentration (5%, 10%, and 30%) of EPP. In the case of the EVA/CB system significant decrease in resistivity is seen above 35 wt% CB. For the EVA/EPP/CB systems, the change in VR is much less pronounced and the electrical performance of this system follows a different trend. Here it must be noted that the overall amount of CB in the system is kept constant with respect to the amount of EVA, at a ratio of 60/40. Therefore by observing that the overall resistivity of the composition remains relatively unchanged with increasing EPP content as shown in Fig. 1, one can assume that the majority of the filler remains localised in the EVA phase [21–29].

By reducing the conductive filler concentration, an increase of melt flow rate can be observed for both systems in Fig. 2, where the melt flow rate for the EVA/CB materials and the blend compositions as a function of filler content are reported. However, the effect is much more pronounced in the EVA/EPP/CB blends due to the high melt flow rate (MFR) of the EPP component. Consequently the latter acts like a lubricant shifting the MFR vs. CB content curve towards lower viscosity values in comparison to the equivalent EVA/CB curve. This is more clearly seen in Fig. 3 where the MFR is shown vs. VR: at the same level of resistivity, flowability is increased of up to 2 order of magnitude.

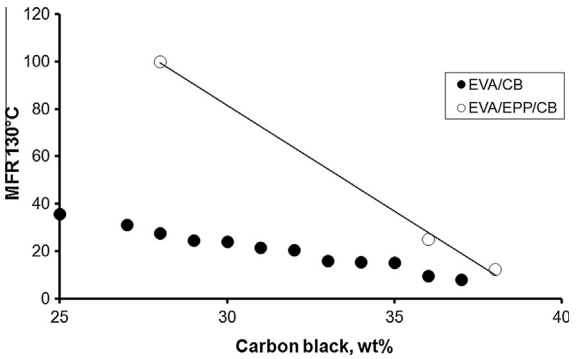

Fig. 2. Melt flow rate as a function of CB loading for a system containing only EVA/CB and EVA/EPP/CB. Lines are a guide to the eye.

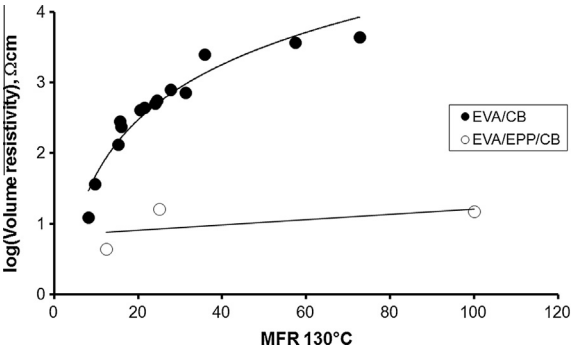

Fig. 3. Melt flow rate as a function of volume resistivity for a system containing only EVA/CB and EVA/EPP/CB. Lines are a guide to the eye.

Alternatively, the results of Fig. 3 shows that a decrease in volume resistivity, for the same MFR, of more than two orders of magnitude can be achieved by adding an additional EPP phase. Furthermore our results indicate that practically constant VR for the blends can be obtained while the MFR can be varied by approximately five times, from 20 to 100 g/10 min. It is also important to note that for the high MFR compositions the overall CB content can be reduced to a level of 28 wt% still achieving good electrical performance. Comparing to Fig. 1, the EVA/CB system is still above the percolation regime at this level of CB content. These changes indicate that there are important morphological differences between the standard EVA/CB system and the materials where EPP is included. Thermal analysis was performed to gain more insight about the overall morphology, while AFM allowed us to highlight differences on microscale.

The DSC results obtained for the samples used in this study are shown in Fig. 1 and Table 4.

Filler introduction alters indeed the crystallization kinetics and likely morphological characteristics of the material. Mixing EVA and EPP gives two crystallisation peaks, since the two materials are immiscible, that are linked to the EVA-rich and EPP-rich phases. However, the data is not a simple superposition of the two phases. Instead we observe an increase in the crystallisation temperature for the EVA, but a reduction in the crystallisation temperature for the EPP (for the blend systems). The peak related to EPP is shifted and its symmetry is lost when adding EVA, middle thermogram in the upper part of Fig. 4. This suggests mutual interaction between EVA and EPP. The lost symmetry or even the almost splitting of the crystallization peak of EPP indicates a different crystallization kinetics within the EPP phase, i.e. the creation of EPP1 and EPP2 phases as it will be shown in the following with microscopy. This is also visible in the thermograms on the bottom of Fig. 4, although this is more difficult to highlight due to the blend compositions, where EPP amounts to down to 5% only.

The blends studied in this work are extensively mixed and we can investigate the preferred location of the carbon black particles given enough mobility using the concepts of polymer miscibility. In other words carbon black particles will either mix with the polymer or phase separate creating an additional segregating phase. Obviously the term "mix" in this case is used loosely, meaning that carbon black particles will be randomly distributed in one or more

Table 4
Crystallisation, glass transition, melting temperatures and melting enthalpy obtained with DSC.

Sample	T_{c1} (°C)	T_{c2} (°C)	T_m (°C)	ΔH_m (J/g)	T_g (°C)
EVA/CB	67		80	64	
EVA/5%EPP/CB	67	31	79	66	−30.3
EVA/10%EPP/CB	65	30	76	62	−29.8
EVA/30%EPP/CB	63	34	77	60	−27.5
EVA	61		80	106	
EPP		43	80	36	−27.0
EVA/EPP	63	34	81	69	

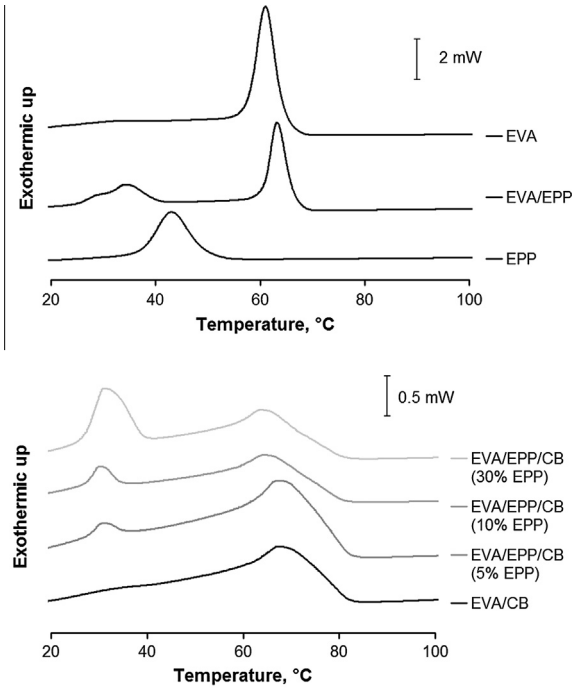

Fig. 4. DSC thermograms for the different compositions used in this study. The curves have been offset to help the reader.

of the polymeric phases in the system. Having said that, one can argue that the specific interactions between the filler and the polymer segments will be manifested in similar ways as the cross-term interaction between two polymers in the case of the standard polymer miscibility treatment.

Thus we can conclude that there is some interaction between the two phases, although they retain most of their bulk properties in the blend. Introducing CB gives a significant increase in crystallisation temperature T_C for the system with pure EVA as the base matrix, but adding also EPP systematically depletes the crystallisation temperature of the EVA/CB-phase. The melting temperature is instead very similar for EVA and EVA/CB, while there is a tendency of a small reduction with inclusion of EPP although a clear trend was not observed.

Increase of the EPP content leads to a decrease in glass transition temperature indicating an increase of mobility in the EPP-rich areas of the matrix. Furthermore the increase of the fraction of EPP in the system tends to move the glass transition closer to the value for pure EPP (−27.0 °C) as seen for the compositions containing 30% EPP (−27.5 °C). Therefore we can see that the change in glass transition is not due to the CB loading hence allowing an assertion, to be confirmed by SEM and AFM in the following, that CB localises in the EVA phase and not in the EPP.

The system EVA/EPP(10%)/CB was imaged with SEM after staining the sample with RuO_4 as reported in Fig. 5. Parts of the sample were not stained, i.e. note in particular the black regions. These do not contain CB, suggesting that the blend comprises a EPP phase free from CB although it was not possible to identify it at this stage. The SEM images

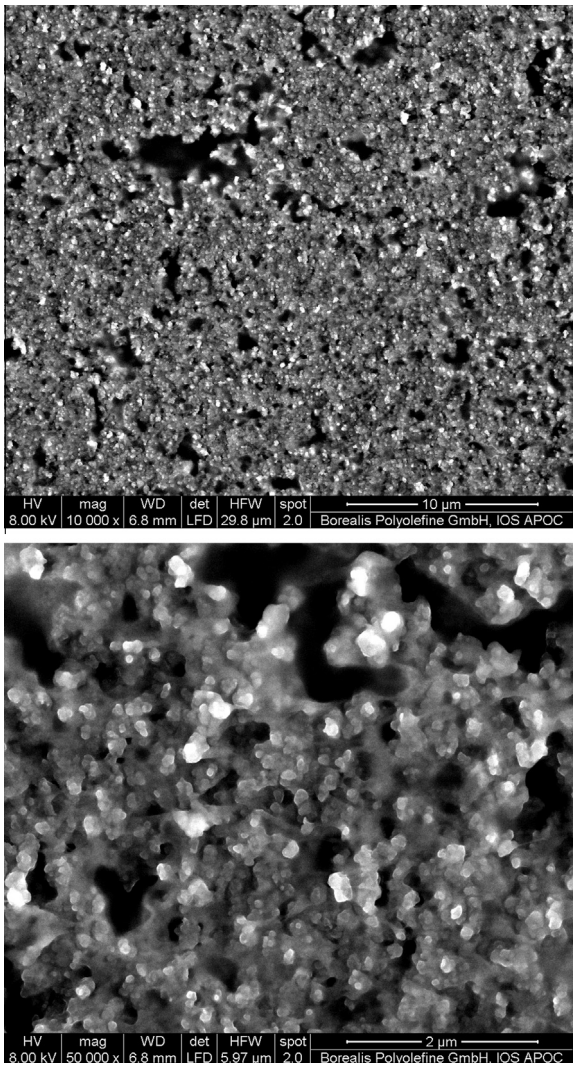

Fig. 5. SEM images after RuO_4 staining of the system EVA/EPP(10%)/CB. Note the dark, unstained areas.

however are not conclusive to discuss in detail phase separation or partial miscibility of EVA and a possibly second phase developed by EPP, since apparently RuO_4 staining is not selective for this purpose and confounds EVA, CB, EPP.

In Fig. 6 the AFM phase lag images can be seen for the pure EVA and EPP samples. Since the phase images are only a relative and qualitative measurement of surfaces' properties [30], special care was taken to imaging the samples with the same cantilever, laser alignment, free oscillation amplitude, set point, minimising the number of collected images to avoid tip contamination and blunting, and so forth. The images of the pure EVA and EPP materials in Fig. 6 are reported together with the phase lag distributions that, given the effort to keep everything as constant as possible, are believed to provide representative information of how the two materials would appear in the blend. This is obviously not fully correct, and this point will be addressed in the following. It can however be appreciated

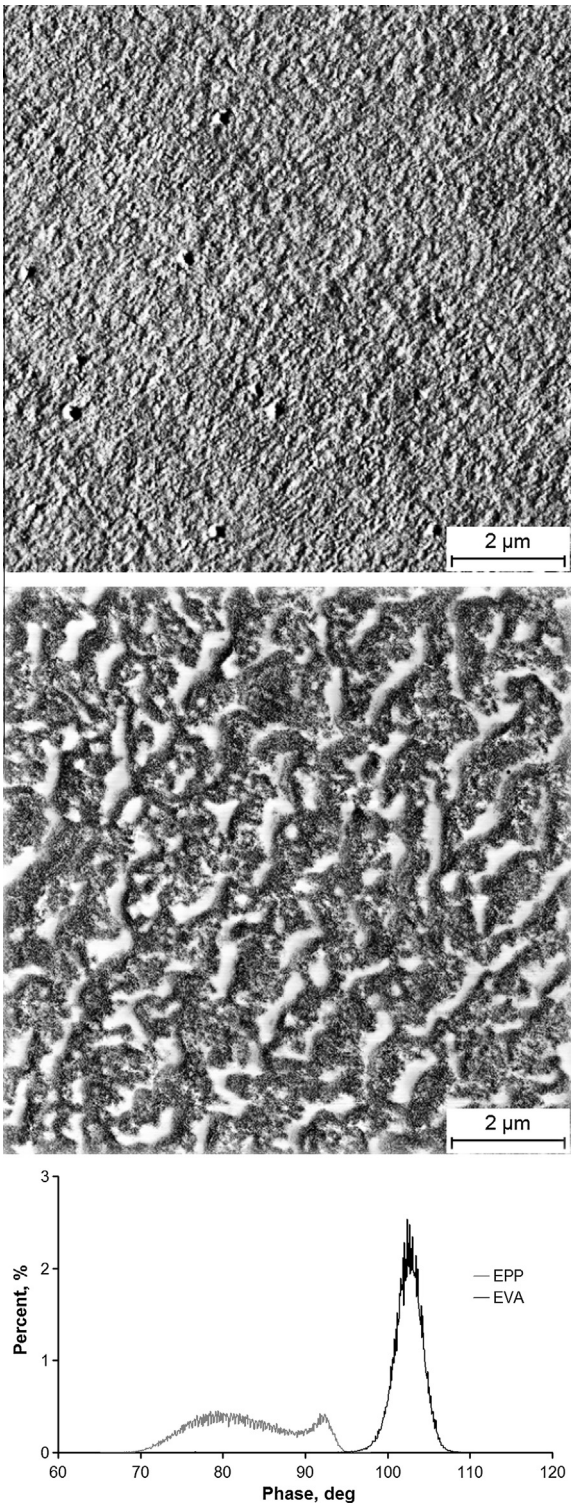

Fig. 6. AFM phase images of the EVA sample, on the top, and of the EPP sample, in the middle. The colour scale is different for the two images in order to allow visualisation of details. On the bottom, the respective phase lag distributions are shown: grey for EPP, black for EVA (For interpretation of the references to colour in this figure legend, the reader is referred to the web version of this article.)

from the histogram that the EVA sample gave a higher phase lag, the phase lag distributions being completely separated hence suggesting that phase images would be able to image the single components clearly, at least in the case of a blend of nonmiscible components. The EPP sample, on the other hand, shows phase separation.

Furthermore the AFM images of the pure EPP in Fig. 6 confirm a phase separation between the propylene-rich part (EPP1) and the ethylene-rich (EPP2) in a manner representing the microphase separation in block copolymers. Due to the chemical similarity between the ethylene repeating units component of EPP and EVA (the latter approximately 80% ethylene), a certain level of mixing between these components could be expected as observed by the DSC results. Nevertheless this interaction and miscibility should be limited as the amount of ethylene in EPP is only 8.6 wt% and furthermore the ethylene part of the EPP is physically connected to the propylene part, thus forcing only a certain level of mixing (albeit in the microscopic level) between the two EPP components.

AFM images of the blends EVA/EPP(10%)/CB and EVA/EPP(30%)/CB are shown in Fig. 7. Although the obvious issue of representativity of microscopy images holds in this case, it appears that regions with lower phase lag can be clearly identified as somewhat related to EPP content. These areas appear similar to the AFM images of pure EPP in Fig. 6, compare in particular to the large darker areas of Fig. 7, and to the unstained areas of SEM images in Fig. 5. Results not shown here confirmed the phase separation of a blend of EVA and EPP. However the solidification in presence of large amount of CB, which is also preferably mixed with EVA phase only, gives rise to a different morphology.

The images of the blends in Figs. 7–9 show a complex morphological structure with areas that appear, given the contrast chosen by the authors, dark grey, light grey, and white.

Building in particular on the results of the electrical characterisation, we can state that carbon black particles are preferentially located in the EVA since the resistivity of the blends does not depend on the EPP content. This is also in agreement with previously reported results [21,31]. Comparing phase images to topography in Fig. 8, one would notice that holes or bumps are very often found corresponding to the white areas in the phase images, suggesting that CB particles were removed upon cryocutting or pressed into the matrix due to their higher hardness, in both cases leading to an overestimation of EVA content.

The content of the white phase in the AFM images of EVA/EPP(10%)/CB blends was evaluated with SPIP software, resulting in ~20–30% at the different magnifications examined. This evaluation conflicts with the expected EVA content of 54% in the blend, see Table 3. Since CB is located in EVA and contributes to mechanically reinforce it, we can conclude that the grey observed areas are to be attributed to EVA/CB. The content of the white phase in the images of EVA/EPP(30%)/CB was instead comparable with the EVA content, i.e. ~40%. However this latter value overestimated the EVA alone content, as mentioned above.

Traditionally carbon black localisation is considered to be influenced by surface tension between the different phases, although parameters like polarity, viscosity and chain architecture are considered to play an important role [19]. In the case of thermodynamic factors affecting the preferential location, the basic need is for the viscosities of the two polymers to be relatively similar [19,32]. By the term thermodynamic factors we refer to all types of enthalpic interactions between the polymer chain and the CB surface (or particle) in a manner similar to the χ parameter in the standard polymer miscibility cases. In our study the viscosities of the two polymers differ, thus opening the possibilities for other parameters except thermodynamics to affect the filler arrangement and localisation. It has been reported [33] that longer and linear polymeric chains are better packed on graphite surface in comparison with shorter chains and chains with bulky side groups. In our case EVA has a network structure with long

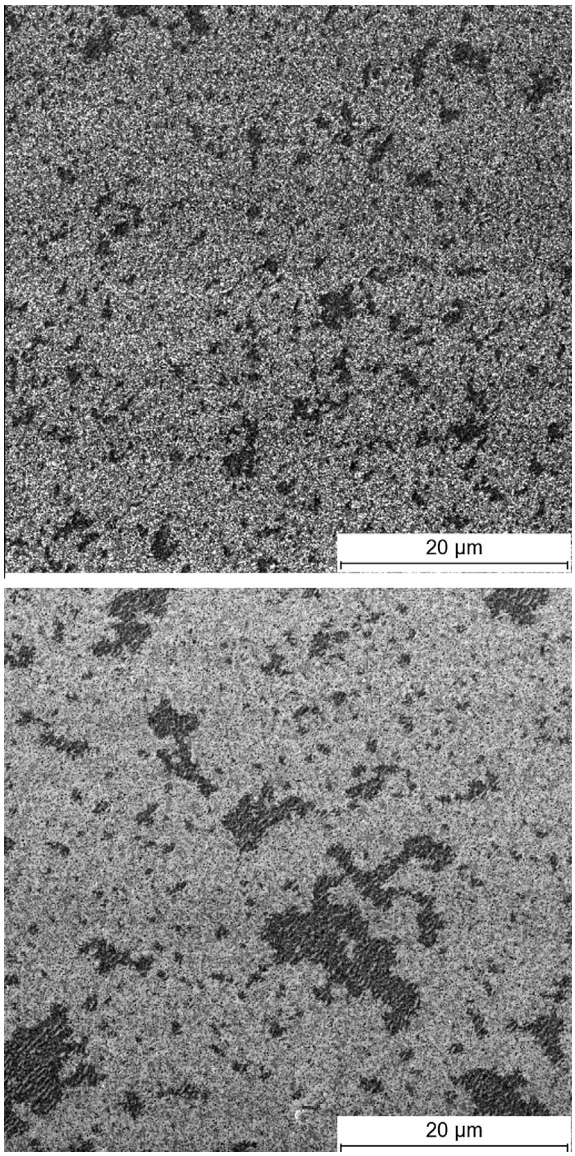

Fig. 7. AFM phase images of the blends EVA/EPP(10%)CB on the top, and EVA/EPP(30%)CB on the bottom.

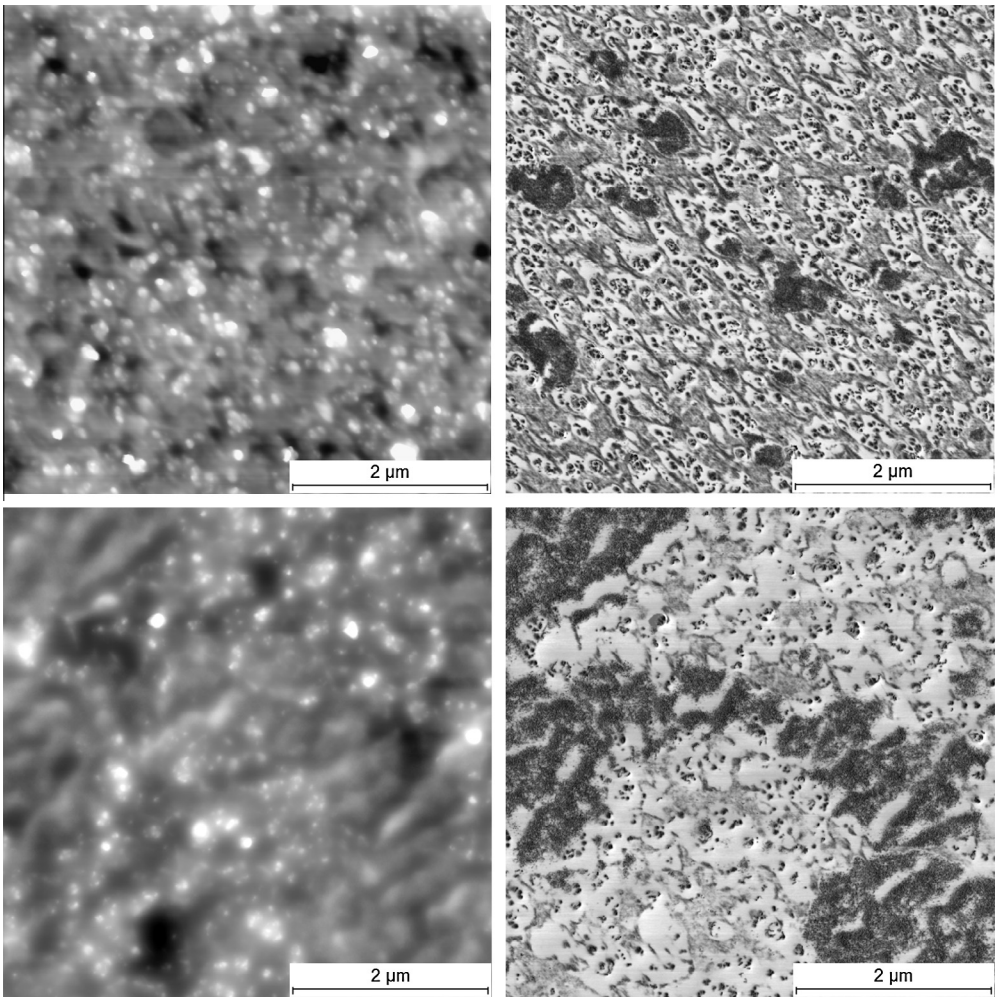

Fig. 8. Topography and phase images of the EVA/EPP(10%)/CB, on the top, and EVA/EPP(30%)/CB blend on the bottom.

chains and a large number of branches, whereas EPP has a more linear chain. Therefore CB localisation will be a competition between thermodynamic properties, closeness of packing on the CB surface and polar interactions between the different components. EVA exhibits polarity, therefore it is expected that hydrogen bonds will be created between the NO_X groups on the CB surface and the atoms on the EVA backbone. This type of interaction is much stronger than the thermodynamic ones and based on our results it appears that it neglects the large viscosity difference between the two polymer phases.

It remains to be clarified whether EVA is partially miscible with EPP, as suggested by thermal analysis. The phase images of the blends EVA/EPP(30%)/CB and EVA/EPP(10%)/CB were saturated in red at high phase lags until covering the clearly visible white network. When this was done, also areas within the EPP1 phase were covered, suggesting that EVA and the ethylene-rich part of EPP are mixed thus tentatively visualising the phenomenon observed with thermal analysis where a significant decrease of the crystallization temperature was measured for the EPP phase in the blend with EVA.

The EPP1 phase, CB-excluded regions, act as insulators since it is energetically not favourable for CB particles to localise in those regions. Areas where the EPP2 phase is partially mixed with EVA probably further increase electrical conductivity by (i) impeding the formation of CB agglomerates and (ii) forcing the EVA phase to a finely dispersed morphology which boosts the ability to form a percolating network.

4. Summary

In this study we have introduced a third component into a system of EVA and carbon black. The macroscopic measurement confirms that VR and MFR, two of the key designing properties of conductive polymer composites, can be controlled by using the conceptual idea of immiscible blends. Our data demonstrate the large range of flowability that can be accessed, while keeping the electrical properties practically constant.

The partial immiscibility between the two polymers creates a multiple phase system in which the conductive

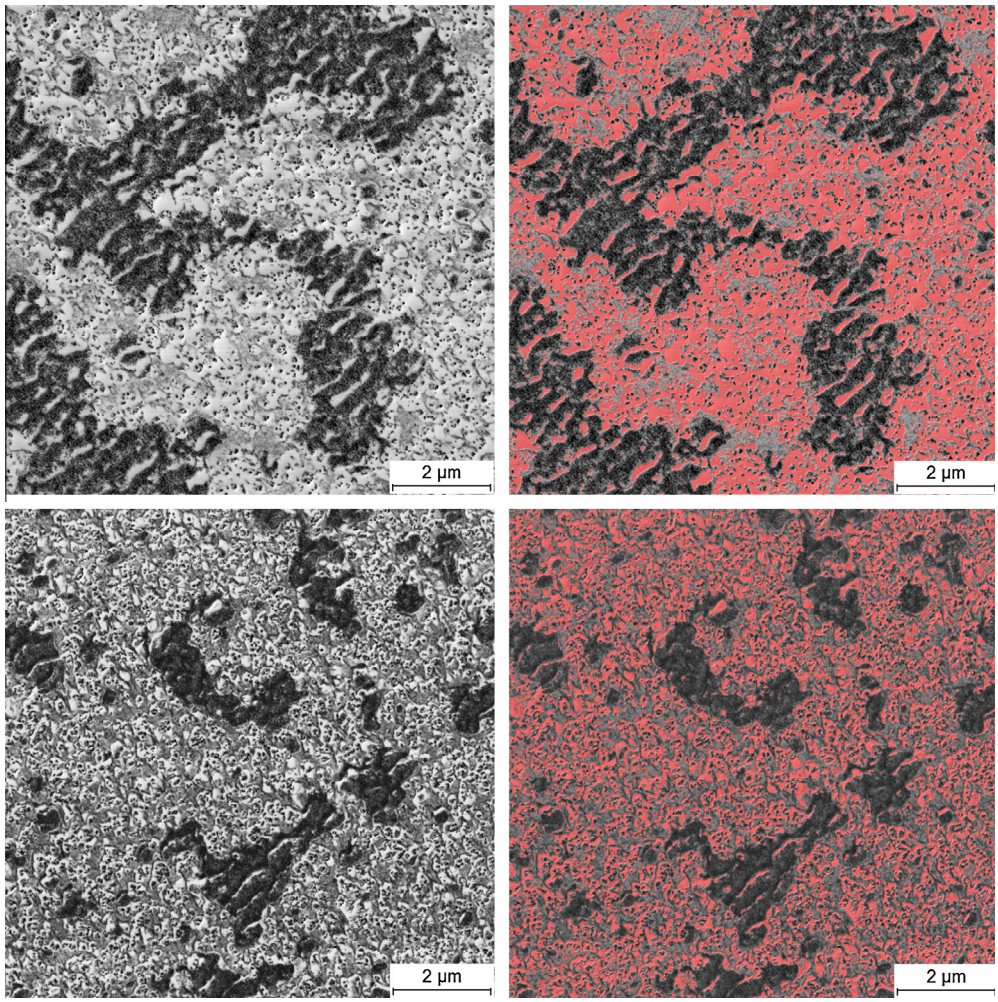

Fig. 9. AFM phase images of the EVA/EPP(30%)/CB on the top, and of EVA/EPP(10%)/CB on the bottom. Parts of the images have been saturated on the right, to tentatively highlight EPP2/EVA phase as discussed in the text.

filler exhibits preferential localisation in the EVA phase. This localisation constrains the mobility and dynamics of the EVA chains. Furthermore it has been reported that in the presence of conductive filler, the liquid polymer tends to exhibit reduced mobility [34]. This is thought to arise from the sheer size difference between the filler and the average polymer chain. In other words the polymer chains are packed tightly on the CB surface, thus losing their mobility and adopting a different conformation.

The CB particles in the matrix do create a conductive pathway, given the low values of VR in Fig. 1, also inhibiting their agglomeration. These agglomerates would be totally surrounded by polymer, acting like an insulating barrier and thus not contributing to the electrical conductivity.

The conductive particles are of similar size or larger than the polymer chains in question and that will limit the possible ways they can pack in the melt. This limitation is manifested by the traditionally observed isolated CB agglomerates and the nature of the percolation network in the case of current flow through the material. By adding another material that is almost exclusively free from the conductive filler we are restricting the volume available to the EVA and EVA/CB phases. This limitation and the existence of such a large surface area of the filler appear to change the morphological characteristics of the system. These changes are manifested by the broadening of the crystallisation peak and the overall level of crystallinity that is reduced from approximately 27% (in the case of pure EVA) to 17% (in the case of EVA/CB).

We have shown that by altering the polymer composition the ability to process and extrude the material can be fine-tuned while keeping the electrical properties constant. Combined with the detailed knowledge of morphology this open ups new possibility of specially designing polymer-based blends for conductive applications.

Acknowledgements

We would like to thank Håkan Svens, Urban Andreasson and Rey-Ove Karlen for all their help and ingenuity during sample preparation, Magnus Person Alfredsson for his help

with the DSC measurements and Matt Parkinson and Christian Piel for their support during material characterisation. We would also like to thank Jenny-Ann Östlund, Ola Fagrell and Karl-Michael Jäger for all the stimulating discussions and suggestions. Finally, we would like to thank the anonymous referees for their input, which allowed us to greatly improve the manuscript.

References

[1] Medalia AI. Rubber. Chem Technol 1986;59:432.
[2] Kirkpartick S. Rev Mod Phys 1973;45:574.
[3] Lux FJ. Mater Sci 1993;28:285.
[4] Zallen P. The Physics of amorphous solids. New York: Wiley; 1983.
[5] Chodak I, Omastova M, Pionteck J. J Appl Polym Sci 2001;82:1903.
[6] Xia J, Pan Y, Shen L, Yi XS. J Mater Sci 2000;35:6145.
[7] Bigg DM, Stutz DE. Polym Compd 1983;4:40.
[8] Lundberg B, Sundqvist B. J Appl Polym Sci 1998;60:1074.
[9] Miyashita Y, Makishi Y, Kato H. Annual report – conference on electrical insulation and dielectric phenomena; 1993. p. 678
[10] Yi XS, Wu G, Ma D. J Appl Polym Sci 1998;67:131.
[11] Sumita M, Abe H, Kayaki H, Myasaka K. J Macromol Sci Phys B 1986;31:6724.
[12] Tang H, Chen X, Tang A, Luo Y. J Appl Polym Sci 1996;59:383.
[13] Hartlein R, Orton HE, Long-life XLPE-insulated power cables; October 2006.
[14] Hogan JD. The Vanderbuilt rubber handbook. 13th ed. In: Ohm RF, editor. New York: Vanderbuilt Company; 1990.
[15] Suzuki YY, Heeger AJ, Pincus P. Macromolecules 1990;23:4730.
[16] Levon K, Margolina A, Patashinsky A. Macromolecules 1993;26:4061.
[17] Zhang QH, Chen DJ. J Mater Sci 2004;39:1751.
[18] Sumita M, Sakata K, Asai S, Miyasaka K, Nakagawa H. Polym Bull 1991;114:4971.
[19] Zhang MQ, Yu G, Zeng HM, Zhang HB, Hou YH. Macromolecules 1998;31:6724.
[20] Gubbels F, Jerome R, Vanlathem E, Deltour R, Blacher S, Brouers F. Chem Mater 1998;10:1227.
[21] Huang J-C, Wu CL, Grossman S. J Polym Eng 2000;20:213.
[22] Zhang Q-H, Chen D-J. J Mater Sci 2004;39:1751.
[23] Li Q, Park OK, Lee J-H. Adv Mater Res 2009;79–28:2267.
[24] Foulger SHJ. Polym Sci B Polym Phys 1999;37:1899.
[25] Park S-J, Kim H-C, H.-Y. Kim. J Colloid Interf Sci 2002;255:145.
[26] Yang Q-Q, Liang J-Z. J Appl Polym Sci 2010;117:1998.
[27] Huang JC, Wu CL. Adv Polym Technol 2000;19:132.
[28] Huang JC, Wu CL, Burke DM. Int J Polym Mater 2002;51:1095.
[29] Huang JC, Huang HL. J Polym Eng 1997;19:132.
[30] García R, Pérez R. Surf Sci Rep 2002;47:197.
[31] Gupta AK, Ratnam BK, Srinivasan KR. J Appl Polym Sci 1992;46:281.
[32] Sumita M, Sakata K, Asai S, Miyasaka K, Nakagawa H. Polym Bull 1991;25:265.
[33] Kern HE, Findenegg GH. J Coll Int Sci 1980;75:346.
[34] Aling I, Pötschke P, Lellinger D, Skipa T, Pegel S, Kasaliwal GR, et al. Polymer 2012;53:4.